3D printing fabrication of Ethylene-Vinyl Acetate (EVA) based intravaginal rings for antifungal therapy

Sofia Moroni[1], Francesca Bischi[1], Annalisa Aluigi[1], Raffaella Campana[1], Mattia Tiboni[1*], and Luca Casettari[1]

[1]*Department of Biomolecular Sciences, University of Urbino Carlo Bo, Piazza del Rinascimento, 6, 61029 Urbino (PU), Italy.*

Abstract

Vulvovaginal candidiasis is a vaginal infection that affects women of reproductive age. Its first-line treatment consists in topical applications of conventional drug formulations (*e.g.*, creams and pessaries) containing imidazole drugs. However, the high frequency of administration and recurrences negatively impact patients' well-being. In this context, intravaginal rings (IVRs)offer the possibility of controlled local drug delivery with one single application, thus possibly increasing patient compliance. This project aimed to fabricate, via 3D printing (3DP), IVRs to highlight the potential application of these medical devices for antifungal therapy. Ethylene-Vinyl Acetate copolymer (EVA) was chosen as the matrix for the medical devices, and bifonazole (BFZ) and clotrimazole (CTZ) was compared as antifungal drugs. The IVRs were computer-designed accordingly to standard measures and printed with the Fused Deposition Modeling (FDM) technique, coupled with Hot-Melt Extrusion (HME). The resulting medical devices were physico-chemically characterized usingFourier Transformed Infrared spectroscopy (FTIR), and the thermal behavior was investigated with Thermogravimetric Analysis (TGA) and Differential Scanning Calorimetry (DSC). In addition, the drug release profile was evaluated in 50% Ethanol in water at 37°C, showing a sustained release over a week. To evaluate the antifungal activity, an *in vitro* time-kill assay was performed against *Candida albicans* for 7 days, exhibiting a complete growth inhibition after 4 days for the3D printed IVRs. Overall, this work represents a step forward in the production of 3D printed IVR potentially able to exert antifungal activity with one single application.

*Corresponding author: mattia.tiboni@uniurb.it

Keywords: Additive manufacturing; Fused Deposition Modeling; Hot-Melt Extrusion; Personalized medicine.

1. Introduction

Vulvovaginal candidiasis (VVC) is a frequent and common infection of the vulva and/or vagina predominantly caused by the pathogen fungus *Candida albicans*, or related fungi. After bacterial vaginosis, it is the second most common cause of vaginal infections, affecting millions of women every year (Sobel, 2007). *Candida albicans* is commonly found on the mucous surfaces of the human body, being part of the quiescent flora. However, changes in the environment can promote proliferation and infection development, characterized by the following symptoms including itching, vaginal soreness, irritation, burning, swelling, dyspareunia, external dysuria, and abnormal vaginal discharge (Gonçalves et al., 2016; Gulati and Nobile, 2016). The pathogenesis depends on the virulence of the *Candida* and on the defence mechanisms of the individual. Some predisposing factors and triggering mechanisms have been identified, such as the use of antibiotics, uncontrolled diabetes, use of contraceptives, and hormonal genetic and lifestyle-related factors (Dall et al., 2009; Spinillo et al., 1995; Yano et al., 2019).

The conventional treatment of candidiasis consists in administering antifungal drugs, available in a variety of standard formulations, such as pessaries or creams, for a duration from three to seven days (Johal et al., 2016). Among antifungal drugs, the class of imidazoles is still considered the first-line treatment for *Candida albicans* infections. This class of drugs inhibits the enzyme lanosterol 14-alpha-demethylase, cytochrome P450 dependent, which is essential for sterols biosynthesis.

Moreover, the maintenance regimen is recommended to avoid recurrences and includes oral weekly antifungal drugs for up to 6 months (Farr et al., 2021). Despite the therapeutic advances, the high frequency of treatment administration, the onset of symptoms, and recurrences still impact the psychological well-being of patients (Aballéa et al., 2013; Denning et al., 2018). Thus, finding an efficient strategy is needed. In this context, IVRs can represent an alternative delivery form. IVRs are flexible medical devices that provide a continuous and sustained or controlled local delivery of the drug incorporated, with a single application (Carson et al., 2021). Based on the advantages conferred, such as the safety and the low side effects, IVRs are well-accepted by women (Griffin et al., 2019) being already established for hormonal therapy (Kerns and Darney, 2011). Additionally, their feasibility and efficacy in other applications associated with women's health have been investigated (*e.g.*, as a microbicide against sexually transmitted infections (Malcolm et al., 2016) and as cervical ripening agents (Wang et al., 2018). The materials utilized for the fabrication of IVRs require specific mechanical characteristics such as elasticity and flexibility. The most common materials employed are silicone elastomer and polyurethane (Boyd et al., 2014). Our group has previously demonstrated the possibility to produce antifungal IVRs by 3D printing using

thermoplastic polyurethane (Tiboni et al., 2021). This project aimed to make a step forward on the development of a new generation of vaginal devices using EVA copolymer as matrix exploring also bifonazole as potential drug candidate for this application.

In recent years, thermoplastic EVA copolymers have shown great potential for the manufacturing of sustained-release matrices. EVA is a biocompatible, insoluble, and non-toxic thermoplastic copolymer of ethylene (E) and vinyl acetate (VA), which has FDA approval, and it is a plastic material suitable to produce particularly elastic products, which stand out for their softness and flexibility (Genina et al., 2016; Henderson, 1993). An example of an EVA-based device, that is available on the market, is the contraceptive IVR Nuvaring®, where the active pharmaceutical ingredients (API) (etonogestrel and ethinylestradiol) are homogeneously distributed within the core polymer, which is in turn covered with a rate-limiting drug-free EVA sheet ("NuvaRing® (etonogestrel/ethinyl estradiol vaginal ring) | Official Site,"). However, at present, the application of IVRs for antifungal treatment has been poorly investigated.

The project aimed to additionally explore the possibility of producing 3D printed IVRs for the treatment of recurrent fungal infections, able to efficiently exert antifungal activity with one single application. For this purpose, EVA was selected as supporting polymer, and the efficacy of BFZ and CTZ as API was compared. IVRs were 3D printed with Fused Deposition Modeling (FDM) technique, coupled with HME to produce the filaments needed during the printing process. The advantage on using 3D printing instead of other techniques relies on the possibility to personalize the shape, the dimensions and the dosage of the medical device based on the different patients' needs. Moreover, the 3DP technology has a lower cost compared to industrial production of special vaginal rings. After an initial characterization comprising size, weight, and drug content homogeneity, the chemical composition, thermal studies (*i.e.,* DSC and TGA), and drug release were evaluated. Finally, to assess the antifungal potentiality of the devices, the *in vitro* antifungal activity was investigated against *Candida albicans* for up to 7 days.

2. Materials and methods

2.1 Materials

EVA1070 copolymer (EVA, Ateva®), in micronized powder form was kindly donated by Celanese Corporation (Germany – USA). The key characteristics of the polymer are a VA content of 9%, tensile strength at break of 17-18 MPa, elongation at break of 400-600%, and flexural modulus of 101 MPa. Bifonazole (BFZ) was purchased from BLD pharm (Germany); while clotrimazole (CTZ) was purchased from Tokyo Chemical Industry (Japan). Methanol, Ethanol, Acetonitrile (ACN), Trifluoracetic acid (TFA), sodium chloride, glacial acetic acid, and formic acid were purchased from Merck (Germany). Lactic acid was purchased from A.C.E.F. (Italy). All solvents used were HPLC grade.

2.2 Methods

2.2.1 Preparation of EVA filaments containing BFZ and CTZ by HME

For the fabrication of 3D printed IVRs, FDM feeding filaments were prepared using HME. For this purpose, EVA in micronized form was mixed with 10% w/w of BFZ or 10% w/w of CTZ. Mixture homogeneity was ensured using a mechanical mixer (Galena Top powder mixer, Ataena, Italy) at a constant speed for 30 minutes. The resulting blends were fed in the filament extruder (Noztek Pro HT, 3 mm nozzle, Noztek, UK), equipped with a stainless-steel barrel and screw, and extruded at 170°C for BFZ and 155°C for CTZ. Blank filaments were produced by feeding the extruder with pure EVA and extruded at a temperature of 150°C (Table 1). The final filaments' diameters ranged between 2.75-2.85 mm.

Table 1. Optimization of HME and FDM parameters used during the production of the IVRs.

Material	***Extrusion Temperature (HME)***	***Printing Temperature (FDM)***
EVA	150°C	190°C
EVA + 10% BFZ	170°C	200°C
EVA + 10% CTZ	155°C	190°C

2.2.2 Fabrication of 3D printed IVRs containing BFZ and CTZ by FDM 3D printing

Drug-loaded and blank IVRs were printed with the prepared filaments using an Ultimaker 3 FDM 3D printer (Ultimaker, The Netherlands). The ring model was designed with a CAD-based software and then converted to a print pattern using UltimakerCura5.0 software (Ultimaker, The Netherlands). The printing parameters were set as follows: layer height 0.1 mm with 100% of infill

density and printing speed of 25 mm/s. The printing temperatures, reported in Table 1, were 190°C both for the blank and CTZ-loaded rings, and 200°C for the ring containing BFZ. The build plate was always kept at 60°C.

2.2.3 Characterization of 3D printed IVRs

After printing, the IVRs were weighed and the OD and CSD were measured using a digital caliper (Mitutoyo, Japan), taking care to ensure that the IVRs were not compressed or distorted during measurements. In addition, filaments and the printed rings were observed with a stereo microscope (Nikon SMZ-1, Nikon, Japan).

2.2.3.1 Homogeneous distribution of the drug

To evaluate the homogeneous distribution of the API in the device, different samples were cut from the printed rings and placed in ethanol for 48 hours under gentle stirring. The amount of BFZ and CTZ released was measured by High Performance Liquid Chromatography (HPLC, Agilent 1260 Infinity II, Agilent, USA). The analysis was conducted with a flow rate of 1 mL/min in an Agilent Zorbax Eclipse Plus C18, 150 × 4.6 mm, 5 µm column (Agilent, USA), keeping the analysis system at room temperature. For BFZ, 0.05% TFA in water and 0.1% TFA in methanol (ratio 30:70) were selected as mobile phases; the injection volume was 10 µL and the detection signal was recorded at 250 nm. While for CTZ, a mixture of 0.5% FA in water and acetonitrile (ratio 55:45) were selected as mobile phases and the detection signal was recorded at 230 nm.

Furthermore, the homogeneous distribution of the drug among the IVRs was confirmed using Attenuated Total Reflectance (FTIR, ATR-FTIR, Spectrum Two FT-IR spectrometer with ATR accessory, Perkin Elmer, MA, USA), by comparing the chemical composition of the printed devices with the starting materials. For this purpose, measurements were performed at 450-4000 cm^{-1} with a resolution of 4 $cm^{-1}$and a total of 64 scans.

2.2.3.2 Thermal behaviour

The thermal behaviour of the raw materials and the printed devices was assessed using TGA and DSC.

For TGA, (TGA Perkin Elmer 4000, Perkin Elmer, MA, USA) scans were run from room temperature to 500°C, at a speed rate of 10°C/min under a nitrogen flow rate of 30 mL/min.

For DSC (DSC Perkin Elmer 6000, Perkin Elmer, MA, USA), approximately 3 mg of each sample were placed in aluminium pans and were heated up with a fixed heating rate of 10°C/min from 30 to 200°C, cooled down at a fixed cooling rate of 5 °C/min to -30 °C and heated up again to 200 °C.

All thermal data were analyzed by Pyris Manager software (Perkin Elmer, MA, USA).The crystallinity degree (χ) was calculated according to equation 1.

$$\chi(\%) = [\Delta H_m/(\Delta H_m^*)]*100 \qquad (1)$$

Where the ΔH_m and ΔH_m*are the melting enthalpies of the analyzed sample and the enthalpy of the 100% crystalline polyethylene (ΔH_m*=287.3 J g^{-1}) respectively.

2.2.4 In vitro BFZ and CTZ release study

For the release study, the 3D printed IVRs were placed in sealed glass bottles with 100 mL of release medium (50%Ethanol in water). The bottles were kept at 37°Cunder gentle stirring (100 rpm) for seven days.1 mL of each sample was withdrawn every two hours for the first 6 hours, then every 24 hours, replacing the volume with fresh medium, preheated at the same temperature. The amount of BFZ and CTZ released from the IVRs was measured with HPLC as reported above (section 2.2.3.1). Experiments were conducted in triplicate.

2.2.5 Microbial strain and culture conditions

In this study, the reference strains *Candida albicans* ATCC 10231 was selected. The strain was grown on Sabouraud Dextrose Agar (SDA) plates (VWR, Milan, Italy) at 37 °C for 24 h, while the stock cultures were kept at -80 °C in Nutrient Broth (VWR) with 15% of glycerol.

2.2.6 Minimum inhibitory concentration (MIC) determination of both BFZ and CTZ

The MIC of each drug was determined following the standard micro-dilution method (Espinel-Ingroff et al., 2007). As first, BFZ and CTZ stock solutions were prepared in DMSO of biological grade (2 mg/mL) and stored at 4°C in the dark. *C. albicans* ATCC 10231 was incubated in Tryptone Soy Broth (TSB, VWR) (20 mL) for 24 h at 37 °C. Afterwards, the microbial suspension was spectrophotometrically adjusted ($OD_{600\ nm}$) to 0.13-0.15 corresponding to about 10^6 CFU/mL. Then, 100 µL of this suspension was diluted 1:50 in standard RPMI 1640 medium (Sigma-Aldrich, Milan, Italy) and inoculated into a 96-well plate together with the adequate volumes of BFZ and CTZ solution (0.0625–16 µg/mL). Two rows inoculated with medium without the antifungal agent (control growth) and one with only medium (negative control) were considered. Preliminary tests were performed with DMSO to exclude its possible antifungal activity; in any case, the volume of DMSO never exceeded 5% (v/v). All the plates were incubated at 37 °C and examined after 24 h of incubation. MIC is defined as the lowest drug concentration able to inhibit the visible growth in comparison to the untreated control. The turbidity of the 96-well plate was also measured using a

193 spectrophotometer (530 nm) (Multiskan EX, Thermo Scientific). *C. albicans* ATCC 10231
194 exhibited sensitivity to BFZ and CTZ showing MIC values of 2 and 0.0625 µg/mL respectively.
195
196 *2.2.7 Preliminary anticandidal assay in agar plates*
197 All the formulated IVRs (blank, 10% BFZ, and 10% CTZ) were previously sterilized by UV
198 radiation underflow safety cabinet for 1 hour (30 minutes for each side) and then stored in sterile
199 Petri dishes. The anticandidal assay was performed as previously reported (Tiboni et al., 2021).
200 Briefly, several colonies of *C. albicans* ATCC 10231 were inoculated into TSB (15 mL) and
201 incubated at 37 °C for 24 h. The suspension was then quantified by spectrophotometer as described
202 above and 500 µL of this culture was added to 25 mL of sterile SDA maintained at 50 °C and gently
203 homogenised. At this point, 15 mL were rapidly poured into a petri dish and allowed to solidify for
204 several minutes; the formulated IVR was placed in the centre of the solidified layer and the
205 remaining 10 mL of inoculated SDA were poured to englobe the medical device. This procedure
206 was carried out for each formulated IVR in duplicate. The plates were incubated at 37 °C for 24 h,
207 afterwards the presence of a well-defined zone of growth inhibition visible around each IVR, index
208 of anticandidal activity, was observed and measured.
209
210 *2.2.8 Time-kill assay*
211 In this study, a vaginal simulative medium (VSM)(Kasper et al., 2015)was used to simulate the
212 typical vaginal environment of *Candida* infection. The VSM was composed as follow: bovine
213 serum albumin (18 mg/L), NaCl (3.5 g/L), KOH (1.4 g/L), $Ca(OH)_2$ (0.22 g/L), lactic acid 90% (2.2
214 g/L), glycerol 50% (0.32 g/L), urea (0.4 g/L), glacial acid acetic (1 g/L), glucose (0.5% w/v)
215 adjusted to pH 4.2. VSM was then sterilized by filtration (0.22 µm filters) and maintained at 4 °C
216 before use.
217 The day before the experiments, a series of sterile tubes with 20 mL of VSM were prepared and
218 organized as follow: one tube with 10% CTZ IVR, one tube with 10% BFZ IVR, an done with
219 blank IVR (control). The test organism was incubated in 15 mL of TSB at 37 °C for 24 h and, at the
220 end of the incubation period, the suspension was centrifuged at 3,500 rpm for 10 min, the pellet was
221 resuspended in the same volume of VSM up to a turbidity of ca 10^6 CFU/mL. At this point, 1 mL of
222 the inoculum was added to the different sterile tubes incubated at 37 °C with gentle shaking (100
223 rpm). At established time points (up to seven days: baseline, 24, 48, 72, 96, 120, 144, and 168 h),
224 100 µL aliquots were aseptically removed from each series, diluted in sterile physiological saline
225 solution, and spread in triplicate (10 µL) onto SDA plates. After 24 h of incubation at 37 °C, the
226 plates were observed for CFU/mL enumeration. All the experiments were performed in triplicate
227 using independent cultures.

3. Results and Discussion

3.1 Fabrication and characterization of 3D printed IVRs

3D printed IVRs with 10% BFZ and 10% CTZ were produced by HME coupled with FDM technique. The design was chosen to comply with the already commercialized rings, the sizes of which are 54 mm of outer diameter (OD) and 4 mm of cross-sectional diameter (CSD). Filaments and 3D printed rings were observed with a microscope to ensure the absence of aggregates as shown in Figure1. The blank and loaded filaments and IVRs presented a smooth and uniform surface. In particular, the blank IVRs were clear and transparent, while the drug-loaded IVRs showed, respectively, intense white color for the BFZ IVR, and a white to pale yellow for the CTZ IVR, due to the presence of the drugs, as already noticed during the HME process.

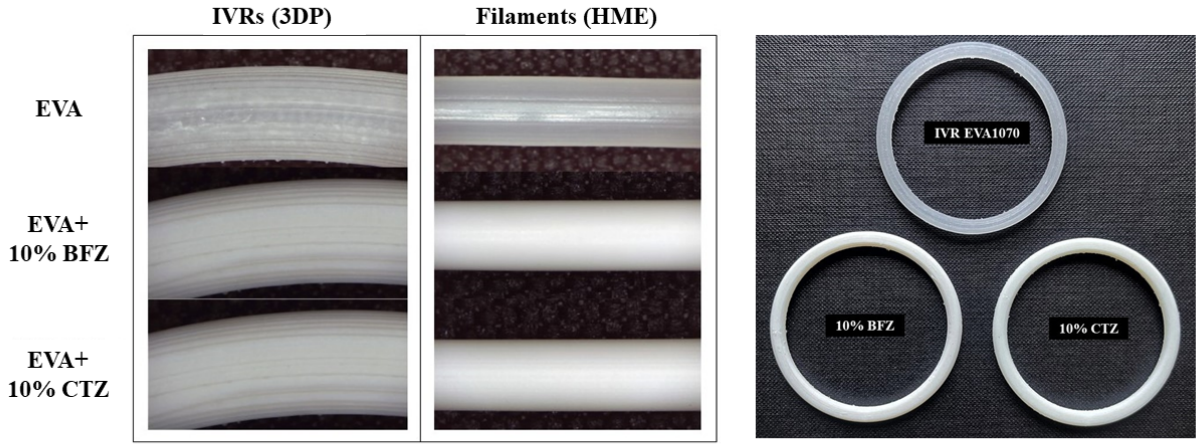

Figure 1 Starting filaments and final IVRs observed with the stereo microscope.3D printed IVRs.

Immediately after printing, the rings were measured for their OD and weighted. The resulting measurements are reported in Table 2. All the manufactured devices were considered dimensionally accurate as they were within the specific acceptance criteria. Moreover, the reproducibility of the printing process was demonstrated.

Table 2. Average dimensional and mass analysis of produced IVRs.

Sample	***Weight (g)***	***OD (mm)***	***CSD (mm)***
EVA	1.832 ± 0.005	53.66 ± 0.017	4.02 ± 0.005
EVA+ 10% BFZ	1.861 ± 0.009	53.12 ± 0.042	4.02 ±0.008
EVA+ 10% CTZ	1.873±0.003	53.12 ±0.023	4.03 ±0.008

3.2 Drug distribution evaluation

ATR-FTIR was performed to investigate the chemical composition of the printed IVRs. The resulting spectra are illustrated in Figure 2. The spectra of the printed devices (EVA + 10% BFZ

and EVA + 10% CTZ) presented the typical peaks of the polymer and the respective drug, suggesting that the physiochemical characteristics of the materials were maintained. Specifically, the characteristic peaks of EVA are at 1243 cm^{-1} (caused by the vibration of C-H), at 1740 cm^{-1} (due to the stretching vibration of C-O), at 2980 cm^{-1} (absorbance associated with -OH group vibrations), and bands at 1117 and 710 cm^{-1} (that reflects the vibrations of C-O and O-C-O groups, respectively) (Agarwal et al., 2022). Regarding the API, numerous absorption bands in the fingerprint region can be observed. Given the chemical similarities, the FTIR spectra are similar. The most intense peaks are attributable to the imidazole ring (1000–650 cm^{-1} and 1680–1640 cm^{-1}) and the benzene rings (1600–1585 cm^{-1}). Specifically, the aromatic cycles stretch at 1570 cm^{-1}, 1487 cm^{-1}, the CH stretches in the 900-700cm^{-1} domain, and 1206$cm^{-1}$the CN stretching. In addition, CTZ shows the chlorobenzene stretch at around 1040cm^{-1}.(Kelemen et al., 2017)(Tonglairoum et al., 2015)

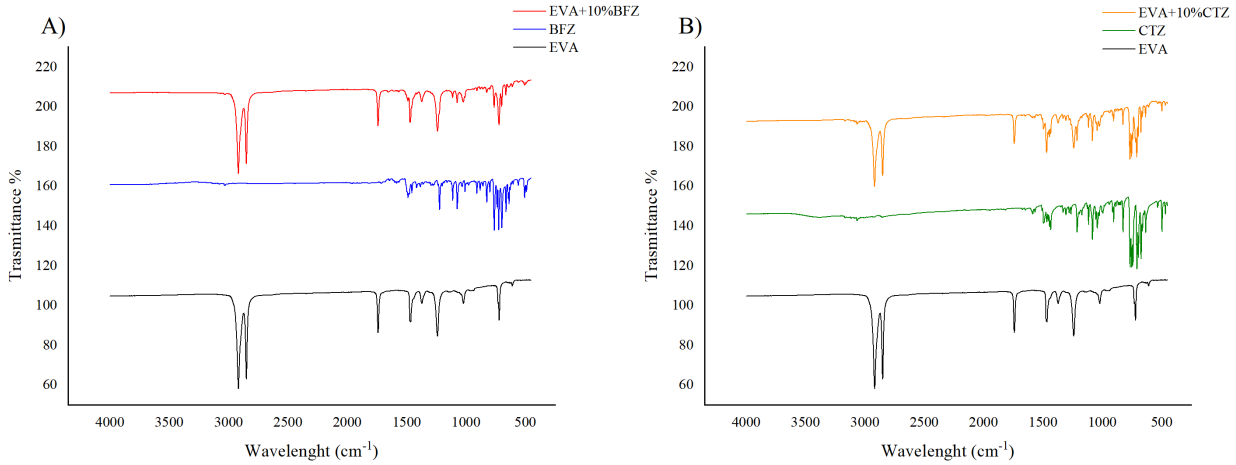

Figure 2.A) FT-IR spectra of EVA, BFZ, and the final BFZ-loaded IVR. **B)** FT-IR spectra of EVA, CTZ, and the final CTZ-loaded IVR.

Moreover, FTIR was employed to assess whether the APIs were uniformly incorporated into the final formulation, by comparing the peaks of random sections of the same sample. For this purpose, the EVA absorption at 2980 $cm^{-1}$was used as reference to normalize and study the samples. As shown in Figure 3, no significant differences in the intensities of the peaks were observed, confirming that the APIs were homogeneously distributed among the devices.

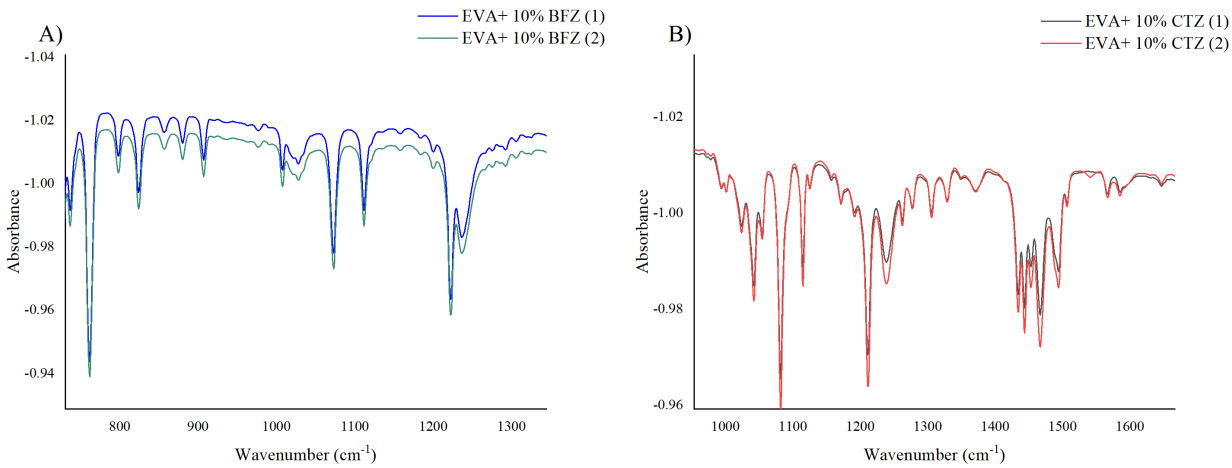

Figure 3. Homogeneous distribution of the sample containing **A)** BFZ; **B)** CTZ evaluated by ATR-FTIR

In addition, to further confirm the homogeneous distribution of the API, different pieces from the same device were cut, weighted, and then placed in ethanol under gentle stirring for 48h to evaluate the drug release. This study showed that no significant differences were present in terms of drug release between different pieces of the same ring.

3.3 Thermal behaviour

Since the production of the IVRs required two thermal processes, the stability of the drugs in the final formulations was evaluated using TGA (Figure 4). In Table 3, the temperatures related to the onset degradation (T_{onset}) and the maximum rate of degradation (T_d) are reported, being evaluated through DTG (Figure 4C-D). Eva showed two steps of degradation: the first T_{onset} approximately at 320.61°C, with a weight loss of just 1.55%, and the second one at 412.69°C, with an additional weight loss of 10.16%, with a $T_d$at483.69°C.TGA measurements of BFZ are shown in Figure 4A, C: at the printing temperature (200 °C), BFZ proved to be thermally stable, starting to slightly degrade at 223.80°C with a weight loss of 1.85%, and the T_d at 329.42°C. The combination of the polymer and the drug leads to higher stability: the first T_{onset} of the final formulation falls at 250.89°C, with a weight loss of 5.15%, while the second step of the degradation is at 408.1°C, with a weight loss of 18.52% from the first T_{onset}; the T_d is recorded at 474.39°C. Regarding CTZ, the degradation occurs at 155°C, being characterized by a weight loss of about 1%, which becomes more consistent at 218.65°C, with a T_d weight loss of 4.67% and the at 302.97°C. As shown in Figure 4B, even in this case, the combination of EVA with CTZ improves drug stabilization. Indeed, the initial degradation temperature of the IVR is higher than the one of the pure drug: the first T_{onset} is at 238.41°C, with a weight loss of 1.17%; and a second T_{onset} at 414.02°C, with a weight loss of 16.51% from the first step and the T_d at 480.63°C. Overall, TGA measurements

confirmed that BFZ and CTZ remained stable at the respective processing temperatures, in addition, results suggest that the polymer displays a protective effect toward the thermal degradation of both drugs. (Garcia Ferreira et al., 2019).

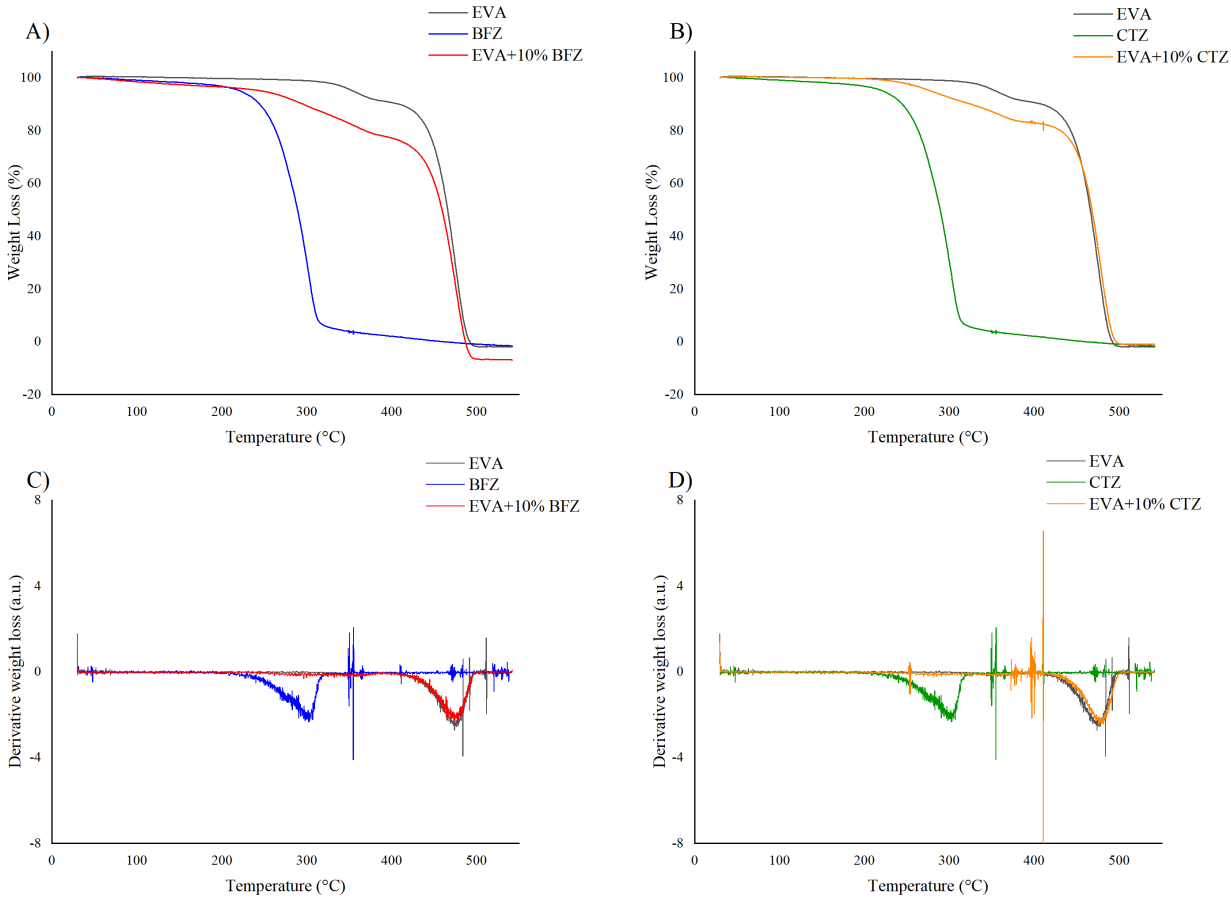

Figure 4.A) TGA of EVA, BFZ, and EVA+10% BFZ; **B)** TGA of EVA, CTZ, and EVA+10% CTZ; **C)** DTG of EVA, BFZ, and EVA+10% BFZ; **D)** DTG of EVA, CTZ, and EVA+10% CTZ.

To investigate the effect of the API on the thermal behaviour of EVA, DSC analysis in the 30-200 °C range was carried out. In Figure 5 the DSC thermograms of the printed samples and the starting materials, are shown. The melting peaks of EVA appear at about 97 °C; while the melting peaks of the BFZ and CTZ fall at 148°C and 145°C, respectively. EVA + 10% BFZ thermograms reveal two endothermic events, one related to the polymer and the second one attributable to BFZ, suggesting that the drug preserves its crystalline structure within the matrix (Figure 5A). On the other hand, in the EVA + 10% CTZ formulation, the characteristic endothermic peak of CTZ disappears (Figure 5B) and this could be attributed to the dissolution of the drug in the polymer or to the formation of an amorphous solid dispersion of the drug in the EVA matrix. Overall, the presence of the API did not affect the crystallinity(χ *(%)*) of EVA.

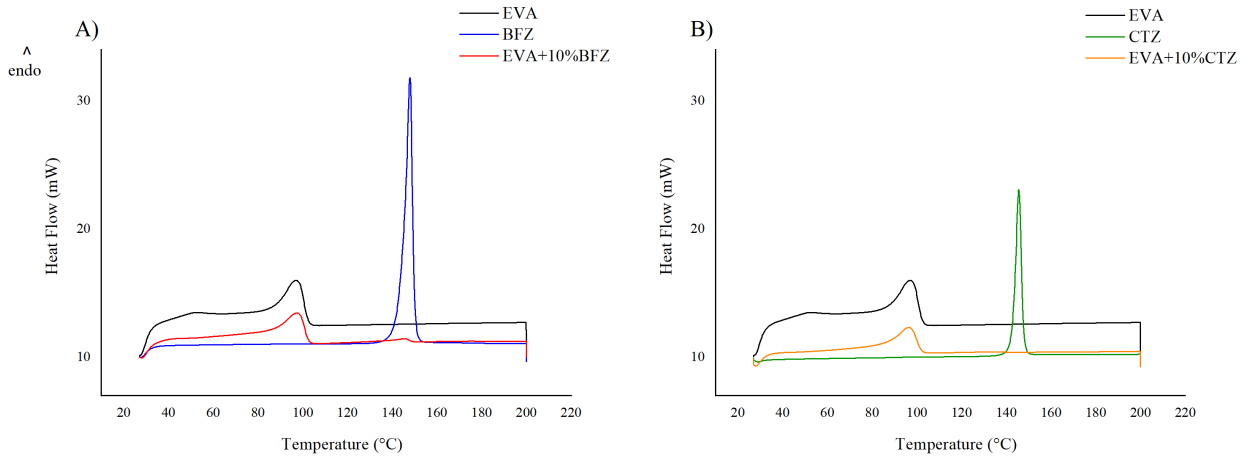

Figure 5. DSC analysis of **A)** EVA + 10% BFZ ring; **B)** EVA + 10% CTZ ring.

Table 3. Melting temperatures, crystallization degree, onset temperatures, and maximum rate of degradation of the samples

Sample	***Tonset (°C)***	***Td (°C)***	***Tm (°C)***	***χ (%)***
EVA1070	320.61	483.69	97	14.2
BFZ	223.80	329.42	148	#
EVA+ 10% BFZ	250.89	474.39	97	14.4
CTZ	218.65	302.97	145	#
EVA + 10% CTZ	238.41	480.63	97	14.3

3.4 In vitro Bifonazole and Clotrimazole release study

One of the key aspects of the application of IVRs as antifungal delivery systems is that, with one application, they provide a controlled and local drug delivery for a prolonged period, positively impacting patients' well-being. Previous studies reported that the release profile from the EVA matrix is affected by several factors, including the crystallinity of the drug and the polymer, the drug loading, and the extrusion temperature. In addition, the release is influenced by the solubility of the drug in the dissolution medium (Genina et al., 2016). Herein, a mixture of 50% ethanol in water was chosen, as solvent/water mixtures have become common for highly water-insoluble drugs and are applied for quality control purposes (Boyd et al., 2019; McConville et al., 2015). Figure 6 shows the cumulative release profiles of the 3D printed 10% drug loaded IVRs. For both IVRs, a burst release was observed; the release of the CTZ-IVR was faster than BFZ-IVR. This can be attributed to the fact that BFZ was in the crystalline form, as shown from the DSC thermograms, resulting in a slower release rate. In addition, higher percentages were detected for the CTZ-IVR: after one week, the release resulted in 34.63 % and 45.64 % of the total amount present in one ring,

for BFZ and CTZ respectively. CTZ-IVR has shown a sustained release of the drug during seven days in the tested media, unlike BFZ-IVR demonstrated a more prolonged release. In Figure 6B, the daily release is reported.For both formulations, the amount of drug released was higher than the MIC values measured for *Candida albicans* (2 µg/mL for BFZ-IVR and 0.0625 µg/mL for CTZ-IVR), suggesting a potential efficacy.

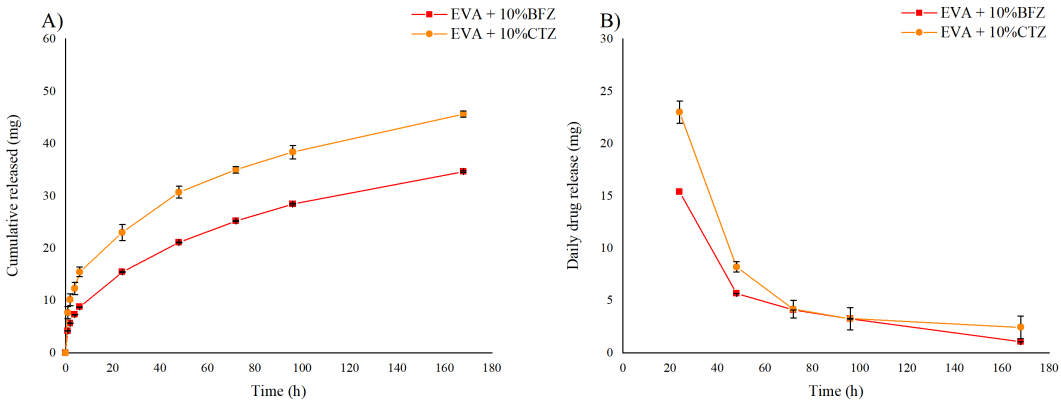

Figure 6. Drug release from 3D printed 10% BFZ-IVR and CTZ-IVR. **A)** Cumulative BFZ and CTZ release; **B)** Daily BFZ and CTZ release.

3.5 Preliminary anticandidal assay in agar plates

The results related to the anti-*candida* activity of IVRs (10% BFZ and CTZ), and relative control (Blank IVR) are presented in Figure 7. As expected, the control EVA-IVR without an antifungal agent showed no growth inhibition, while the presence of the drug-loaded IVRs resulted in a different inhibition of *C. albicans* ATCC 10231 growth. In the plate with 10% BFZ-IVR, the area of growth inhibition after 24 hours was about 1.5 cm (considering the IVR itself). Instead, in the plate with 10% CTZ-IVR, the area of growth inhibition after 24 hours was more remarkable than BFZ, and the growth of *C. albicans* ATCC 10231 was limited to the edge of the plate, away from the IVR, indicating the effectiveness of this type of formulation against the examined microorganism. This test confirmed that CTZ had a better release in 24 hours than BFZ, as detected with the release test (in which we observed that the concentration released after one day is about 15.44 mg for BFZ-IVR and about 23 mg for CTZ-IVR).

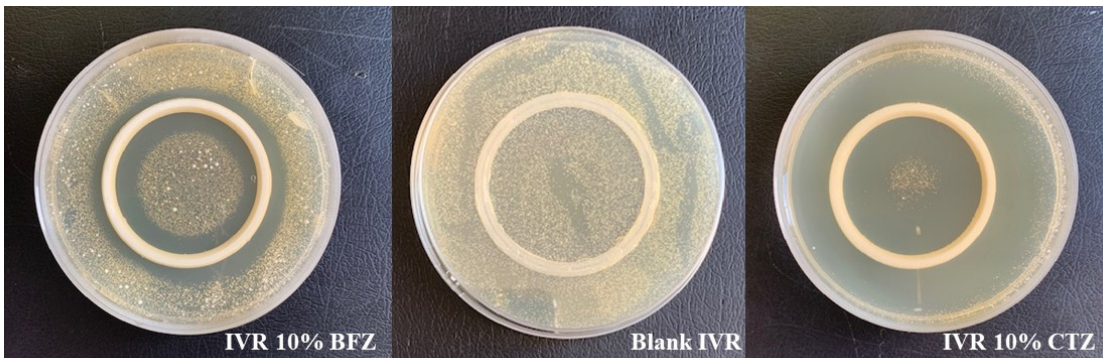

Figure 7. Preliminary antifungal activity of prepared IVRs, assessed by a modified agar-diffusion method.

3.6 Time-kill assay

Time-kill experiments (Figure 8) were performed to confirm the antifungal activity of the different IVRs (plain IVR made with EVA as control and drug loaded IVRs with 10% CTZ, and 10% BFZ) observed in the agar assay. As shown, after 24 h of incubation, the viability of *C. albicans* ATTC 10231 decreased to $5x10^3$ CFU/mL in the presence of 10% CTZ IVR and to $1.6x10^5$ CFU/mL in the presence of 10% BFZ-IVR, while in the control with plain EVA-IVR, the viability increased up to $1x10^7$ CFU/mL. In the following time points (48 and 72 h) a more drastic decrease of the pathogen viability was observed in the presence of 10% CTZ-IVR with values ranging from $1.7x10^2$ to 10 CFU/mL, reaching the complete growth inhibition (no detectable CFU/mL) after 96 h of incubation. With the 10% BFZ-IVR, the decrease of viability was slighter compared to that observed with 10% CTZ-IVR, with CFU/mL values ranging from $5x10^3$ to $1x10^2$ CFU/mL after 48 and 72 h of incubation respectively, reaching no detectable CFU/mL at 96 h. In the control, the growth of *C. albicans* ATCC 10231 continued with increasing CFU/mL values up to 48 h ($5x\ 10^7$ CFU/mL) and then slightly decreased up to $1.2\ x10^6$ CFU/mL after 96 h of incubation. In the final time points (up to 168 h), no CFU/mL were detectable in the presence of the two drug- loaded IVRs, while in the control in which the plain EVA-IVR was present, the viability of *Candida* decreased up to $1x10^3$ CFU/mL. These results are aligned again with the faster release of CTZ compared to BFZ revealed in the drug release studies.

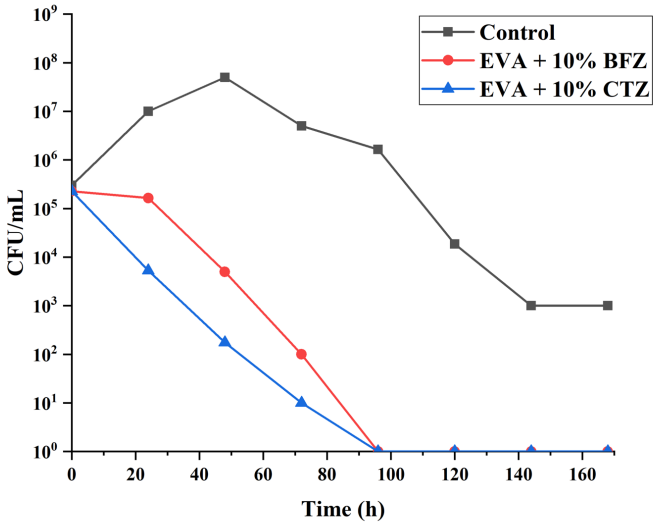

Figure 8. Time-kill assay

4. Conclusions

In this work, we successfully applied FDM 3D printing technology to manufacture drug loaded IVRs using EVA copolymer with 10% of BFZ or CTZ. This confirmed the potential of 3D printing in the formulation of vaginal medical devices with the potential to produce personalized devices in terms of shape, dimension, and dosage with an affordable cost compared to industrial techniques for special rings. The employment of EVA as a matrix polymer allows to control the drug release profile, indeed, results showed a sustained release over a week. The results obtained from the preliminary antifungal activity studies and *in vitro* time kill-assay on *C. albicans,* confirmed the feasibility of applying IVRs as a new treatment strategy against fungal infections. Thus, the printed IVRs can be considered as an alternative to oral antifungals for immediate treatment and/or for maintenance therapy in case of recurrences. In addition, since the common treatment for fungal infections consists of multiple applications of conventional dosage forms, the utilization of an intravaginal device (such as the BFZ- or the CTZ-loaded rings) could improve patient compliance by decreasing the number of applications to one, switching from a daily to a weekly therapy.

CRediT Authorship

Francesca Bischi and Sofia Moroni: Methodology, Investigation, Formal analysis, Data curation, Writing - original draft.

Annalisa Aluigi and Raffaella Campana: Methodology, Data curation, Writing - review & editing.

Mattia Tiboni: Conceptualization, Supervision, Methodology, Formal analysis, Data curation, Writing - review & editing

Luca Casettari: Conceptualization, Resources, Funding acquisition, Project administration, Supervision, Writing - review & editing.

Funding

Sofia Moroni acknowledge Marche Region for the PhD scholarship (Innovative doctoral programme POR Marche FSE 2014/2020 D.R. 354/2020).

This project received support from the European Union – Next Generation EU – VITALITY Project.

Conflict of interest

The authors declare no conflict of interest.

Acknowledgements

We would like to express our sincere gratitude to Celanese for their contribution to this research and for providing Celanese EVA (ethylene vinyl acetate) used in this study as well as the support to article review. Moreover, we acknowledge ITIS E. Mattei (Urbino, PU, Italy) for the utilization of FT-IR instrument.

References

Aballéa, S., Guelfucci, F., Wagner, J., Khemiri, A., Dietz, J.P., Sobel, J., Toumi, M., 2013. Subjective health status and health-related quality of life among women with Recurrent Vulvovaginal Candidosis (RVVC) in Europe and the USA. Health Qual. Life Outcomes 11. https://doi.org/10.1186/1477-7525-11-169

Agarwal, P., Nieuwoudt, M.K., Li, S., Procter, G., Andrews, G.P., Jones, D.S., Svirskis, D., 2022. Exploiting hydrogen bonding to enhance lidocaine loading and stability in a poly ethylene-co-vinyl acetate carrier matrix. Int. J. Pharm. 621. https://doi.org/10.1016/j.ijpharm.2022.121819

Boyd, P., Major, I., Wang, W., McConville, C., 2014. Development of disulfiram-loaded vaginal rings for the localised treatment of cervical cancer. Eur. J. Pharm. Biopharm. 88, 945–953. https://doi.org/10.1016/j.ejpb.2014.08.002

Boyd, P., Variano, B., Spence, P., McCoy, C.F., Murphy, D.J., Dallal Bashi, Y.H., Malcolm, R.K., 2019. In vitro release testing methods for drug-releasing vaginal rings. J. Control. Release. https://doi.org/10.1016/j.jconrel.2019.10.015

Carson, L., Merkatz, R., Martinelli, E., Boyd, P., Variano, B., Sallent, T., Malcolm, R.K., 2021. The Vaginal Microbiota, Bacterial Biofilms and Polymeric Drug-Releasing Vaginal Rings. Pharmaceutics 13. https://doi.org/10.3390/PHARMACEUTICS13050751

Dall, T.M., Mann, S.E., Zhang, Y., Quick, W.W., Seifert, R.F., Martin, J., Huang, E.A., Zhang, S., 2009. Distinguishing the economic costs associated with type 1 and type 2 diabetes. Popul. Health Manag. 12, 103–110. https://doi.org/10.1089/POP.2009.12203

Denning, D.W., Kneale, M., Sobel, J.D., Rautemaa-Richardson, R., 2018. Global burden of recurrent vulvovaginal candidiasis: a systematic review. Lancet. Infect. Dis. 18, e339–e347. https://doi.org/10.1016/S1473-3099(18)30103-8

Espinel-Ingroff, A., Fothergill, A., Ghannoum, M., Manavathu, E., Ostrosky-Zeichner, L., Pfaller, M.A., Rinaldi, M.G., Schell, W., Walsh, T.J., 2007. Quality Control and Reference Guidelines for CLSI Broth Microdilution Method (M38-A Document) for Susceptibility Testing of Anidulafungin against Molds. J. Clin. Microbiol. 45, 2180. https://doi.org/10.1128/JCM.00399-07

Farr, A., Effendy, I., Frey Tirri, B., Hof, H., Mayser, P., Petricevic, L., Ruhnke, M., Schaller, M., Schaefer, A.P.A., Sustr, V., Willinger, B., Mendling, W., 2021. Guideline: Vulvovaginal candidosis (AWMF 015/072, level S2k). Mycoses 64, 583–602. https://doi.org/10.1111/MYC.13248

Garcia Ferreira, P., Guimarães de Souza Lima, C., Noronha, L.L., de Moraes, M.C., Silva, F. de C. da, Lifsitch Viçosa, A., Omena Futuro, D., Francisco Ferreira, V., 2019. Development of a

Method for the Quantification of Clotrimazole and Itraconazole and Study of Their Stability in a New Microemulsion for the Treatment of Sporotrichosis. Molecules 24. https://doi.org/10.3390/MOLECULES24122333

Genina, N., Holländer, J., Jukarainen, H., Mäkilä, E., Salonen, J., Sandler, N., 2016. Ethylene vinyl acetate (EVA) as a new drug carrier for 3D printed medical drug delivery devices. Eur. J. Pharm. Sci. 90, 53–63. https://doi.org/10.1016/J.EJPS.2015.11.005

Gonçalves, B., Ferreira, C., Alves, C.T., Henriques, M., Azeredo, J., Silva, S., 2016. Vulvovaginal candidiasis: Epidemiology, microbiology and risk factors. Crit. Rev. Microbiol. https://doi.org/10.3109/1040841X.2015.1091805

Griffin, J.B., Ridgeway, K., Montgomery, E., Torjesen, K., Clark, R., Peterson, J., Baggaley, R., van der Straten, A., 2019. Vaginal ring acceptability and related preferences among women in low- and middle-income countries: A systematic review and narrative synthesis. PLoS One 14, e0224898. https://doi.org/10.1371/JOURNAL.PONE.0224898

Gulati, M., Nobile, C.J., 2016. Candida albicans biofilms: development, regulation, and molecular mechanisms. Microbes Infect. 18, 310–321. https://doi.org/10.1016/J.MICINF.2016.01.002

Henderson, A.M., 1993. Ethylene-Vinyl Acetate (EVA) Copolymers: A General Review. IEEE Electr. Insul. Mag. 9, 30–38. https://doi.org/10.1109/57.249923

Johal, H.S., Garg, T., Rath, G., Goyal, A.K., 2016. Advanced topical drug delivery system for the management of vaginal candidiasis. Drug Deliv. 23, 550–563. https://doi.org/10.3109/10717544.2014.928760

Kasper, L., Miramón, P., Jablonowski, N., Wisgott, S., Wilson, D., Brunke, S., Hube, B., 2015. Antifungal activity of clotrimazole against Candida albicans depends on carbon sources, growth phase and morphology. J. Med. Microbiol. 64, 714–723. https://doi.org/10.1099/jmm.0.000082

Kelemen, H., Csillag, A., Hancu, G., Székely-Szentmiklósi, B., Fülöp, I., Varga, E., Grama, L., Orgován, G., 2017. Characterization of inclusion complexes between bifonazole and different cyclodextrins in solid and solution state. Maced. J. Chem. Chem. Eng. 36, 81–91. https://doi.org/10.20450/mjcce.2017.1031

Kerns, J., Darney, P., 2011. Vaginal ring contraception. Contraception 83, 107–115. https://doi.org/10.1016/J.CONTRACEPTION.2010.07.008

Malcolm, R.K., Boyd, P.J., McCoy, C.F., Murphy, D.J., 2016. Microbicide vaginal rings: Technological challenges and clinical development. Adv. Drug Deliv. Rev. https://doi.org/10.1016/j.addr.2016.01.015

McConville, C., Smith, J.M., McCoy, C.F., Srinivasan, P., Mitchell, J., Holder, A., Otten, R.A.,

Butera, S., Doncel, G.F., Friend, D.R., Malcolm, R.K., 2015. Lack of in vitro–in vivo correlation for a UC781-releasing vaginal ring in macaques. Drug Deliv. Transl. Res. 5, 27–37. https://doi.org/10.1007/s13346-015-0216-4

NuvaRing® (etonogestrel/ethinyl estradiol vaginal ring) | Official Site [WWW Document], n.d. URL https://www.nuvaring.com/ (accessed 7.28.22).

Sobel, J.D., 2007. Vulvovaginal candidosis. Lancet (London, England) 369, 1961–1971. https://doi.org/10.1016/S0140-6736(07)60917-9

Spinillo, A., Capuzzo, E., Nicola, S., Baltaro, F., Ferrari, A., Monaco, A., 1995. The impact of oral contraception on vulvovaginal candidiasis. Contraception 51, 293–297. https://doi.org/10.1016/0010-7824(95)00079-P

Tiboni, M., Campana, R., Frangipani, E., Casettari, L., 2021. 3D printed clotrimazole intravaginal ring for the treatment of recurrent vaginal candidiasis. Int. J. Pharm. 120290. https://doi.org/10.1016/j.ijpharm.2021.120290

Tonglairoum, P., Ngawhirunpat, T., Rojanarata, T., Panomsuk, S., Kaomongkolgit, R., Opanasopit, P., 2015. Fabrication of mucoadhesive chitosan coated polyvinylpyrrolidone/cyclodextrin/clotrimazole sandwich patches for oral candidiasis. Carbohydr. Polym. 132, 173–179. https://doi.org/10.1016/j.carbpol.2015.06.032

Wang, Y., Boyd, P., Hunter, A., Malcolm, R.K., 2018. Intravaginal rings for continuous low-dose administration of cervical ripening agents. Int. J. Pharm. 549, 124–132. https://doi.org/10.1016/J.IJPHARM.2018.07.053

Yano, J., Sobel, J.D., Nyirjesy, P., Sobel, R., Williams, V.L., Yu, Q., Noverr, M.C., Fidel, P.L., 2019. Current patient perspectives of vulvovaginal candidiasis: incidence, symptoms, management and post-treatment outcomes. BMC Womens. Health 19. https://doi.org/10.1186/S12905-019-0748-8